

New Angles-only Algorithms for Initial Orbit Determination

Gim J. Der

DerAstrodynamics

gim.der@deraastrodynamics.com

Abstract

The extraction of range from optical sensor observation data has always been difficult, expensive and sometimes unreliable. This paper presents three new angles-only algorithms to help mitigate those problems. First, the correct range or root of the Gauss or Laplace eighth-degree polynomial equation is consistently deduced without guesswork for any object in any orbit regime. Second, the Keplerian solution is analytically extended to include perturbations for fast and accurate Initial Orbit Determination (IOD). Using simulated and real data, with or without angular measurement errors, ten numerical examples are presented for comparison. More than a hundred Geocentric and Heliocentric test cases have been independently confirmed by third parties. These analytic angles-only algorithms improve data collection efficiency, catalog maintenance, uncorrelated target cataloging, and ultimately contributing to real-time Space Situation Awareness.

1. Introduction

Initial orbit determination is required for newly detected unknown objects, such as a new foreign launch, an Uncorrelated Target (UCT) or a piece of tracked but un-cataloged space debris. IOD, which requires only sparse data, computes a starting state vector or nominal orbit. Differential Correction (DC), which requires dense data, processes systems and statistical measurement errors to improve a nominal orbit. Dense data collection is time consuming and is not compatible with real-time processing. If IOD fails to initiate tracks, the detected objects will remain as UCT's and uncataloged. As such, they pose a higher threat to space asset than the catalogued objects. In this paper, unless stated otherwise, angles-only algorithm means angles-only IOD algorithm.

Deep space object observations are typically angles-only based. The classical angles-only problem as described in [1] to [21], uses three sets of angles to solve for a Keplerian orbit of an unknown object. All classical methods, which solve for the general solution, unfortunately have two major weaknesses: range guessing to start and Keplerian (2-body) solutions to finish. Range guessing is due to ignoring or not solving the correct real root of the Gauss and Laplace eighth-degree polynomial equations or *the Equations* for short. The Keplerian solutions are due to the difficulty of adding perturbations analytically. Even if the correct initial Keplerian orbit is found, it is often not accurate enough to predict a future acquisition of a Near-Earth object after 24 hours or later. IOD and DC processes have been successfully applied to GEO and Deep Space objects [22] to [24] when a priori knowledge of the "slow moving and high altitude" object is used. Clearly, when no a priori knowledge is assumed, even with the help of powerful computers, the initial orbit of a completely unknown object will be hard to establish with only angles data. This paper presents three new angles-only algorithms to remove these weaknesses.

Proper angles data and an effective angles-only algorithm must work together to produce reasonably accurate IOD nominal orbits. Proper time span and/or angular separation guidelines for Geocentric IOD and Heliocentric IOD are depicted in Figure 1 and summarized as follows:

1. Time and angular spacing: Three sets of angles at reasonably separated time spans of about 10 minutes (Geocentric) and days or months (Heliocentric) are required. A proper angular separation is when the variations of the angular values for two points differ by at least 0.05 degrees.
2. Multi-revolutions: The Gauss or Laplace algorithm is formulated for the three data points within one orbit at least for the first-pass. If the hours- or days-apart data points are indeed within an arc of one orbit, then a good solution may still be found, but there is no guarantee.
3. Angular measurement accuracy: Angles data collected by an operational optical sensor [25] with a Field-of-View resolution of about 2 arc-seconds (0.0005 degrees) provides accurate angles inputs for the Gauss, Laplace and Double-r angles-only algorithms. Error-free inputs imply that all the six angles are accurate with five or more significant digits as described in the Numerical Example Section.

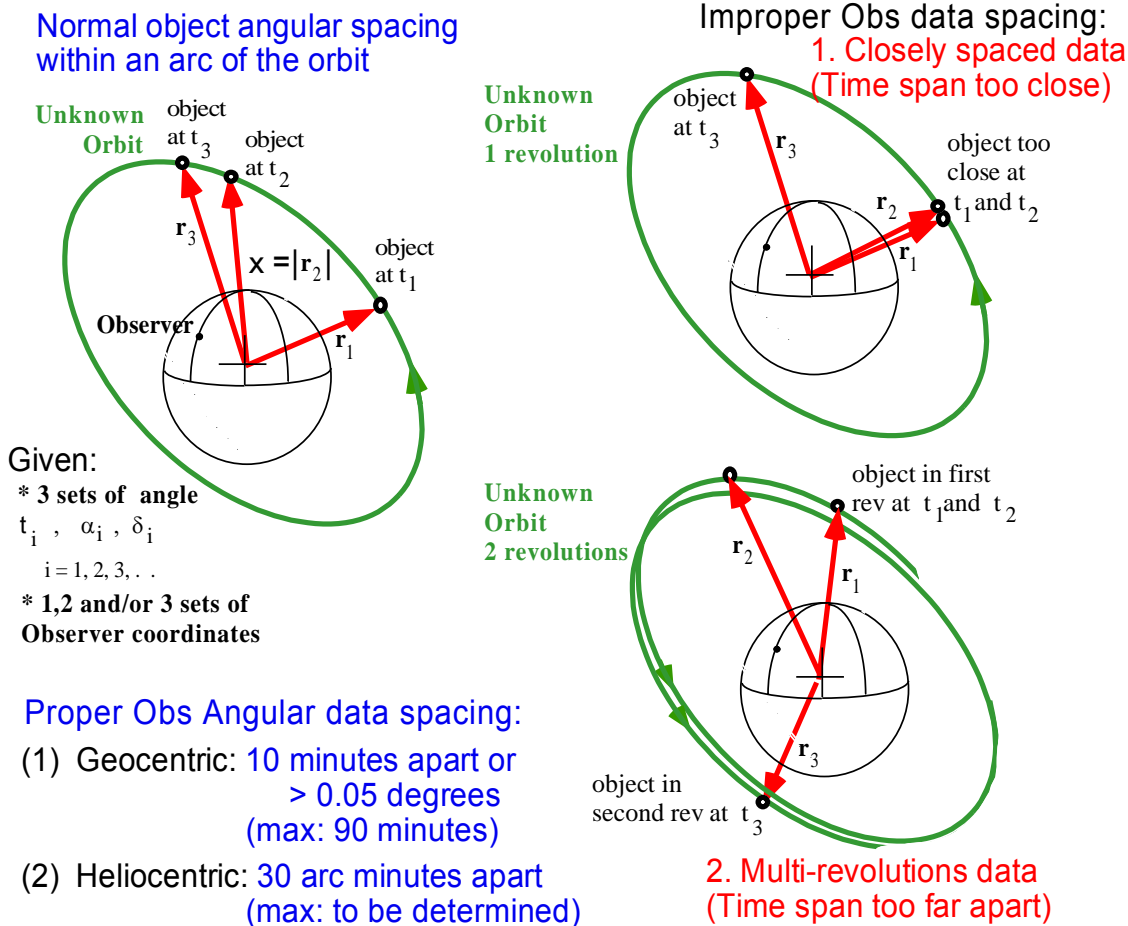


Figure 1. Guidelines for time and angular spacing of angles data

Assuming that proper angles data is given, each correct positive real root of *the Equations* is the initial range estimate at the second time point of the unknown orbit as shown in Figures 1. Theoretically there are eight roots and can be computed by a standard root solver. Charlier applied the Descartes’ Rule of Signs [20] and [21], to the Laplace Equation for Heliocentric objects in 1910 indicating at most three positive real roots. However, the ten numerical examples of this paper show that some of Charlier’s theoretical assertions are incorrect in practice, especially for Geocentric applications. “Selecting the correct root can be very difficult”, as indicated by Vallado [7].

Without guesswork, the new Gauss and Laplace algorithms solve for the correct positive real root of *the Equations* by combining Descartes’ Rule of Signs and the Gauss geometric method. All previous papers may use the same combination, but they start with guessing and/or finish with multiple roots. The algorithms of his paper always provide one correct root. The new Double-r algorithm takes advantage of the range solving solution of Gauss or Laplace to construct two Cartesian position vectors (r_1 and r_3), which in turn transforms the angles-only problem to a Lambert problem. Algorithms that involve range guessing, range hypothesis, partial derivative evaluations, high-order matrix inversions, sensitive iterative methods and unpredictable convergence are avoided.

2. The Correct Root of the Equations of Gauss and Laplace

This section presents a straightforward method to find the correct root of *the Equations*. Since the formulations leading to the *Equations* can be found in many textbooks, they will not be repeated here. Although the Gauss and Laplace formulations are different, the resulting equations have the same form and can be expressed as:

$$f(x) = x^8 + a x^6 + b x^3 + c = 0 \tag{1}$$

where $x = r_2 = |\mathbf{r}(t_2)|$ is the magnitude of the position vector at t_2 . The coefficients a , b , and c , which can be computed from the given inputs to the angles-only problem, are different in numerical values between those of Gauss and Laplace. Theoretically, if the input angles are error-free, then these three coefficients are determined accurately, and the resulting range estimate of Equation (1) is within 99% of the real range at t_2 .

2.1 Descartes' Rule of Signs

Descartes' Rule of Signs states that: If $f(x)$ is a polynomial with non-zero real coefficients, the number of positive roots of Equation (1), cannot exceed the number of changes of signs of the numerical coefficients of $f(x)$. If the observation or the angles data is real, the range x must be positive. There are only four terms in Equation (1), and the coefficient c is always negative. Therefore, at most three changes of signs can occur, implying at most three positive real roots. If the coefficients indicate one positive real root, the correct value of x can be found without guesswork as in Section 2.3, and the Gauss geometric method described in Section 2.2 may be skipped.

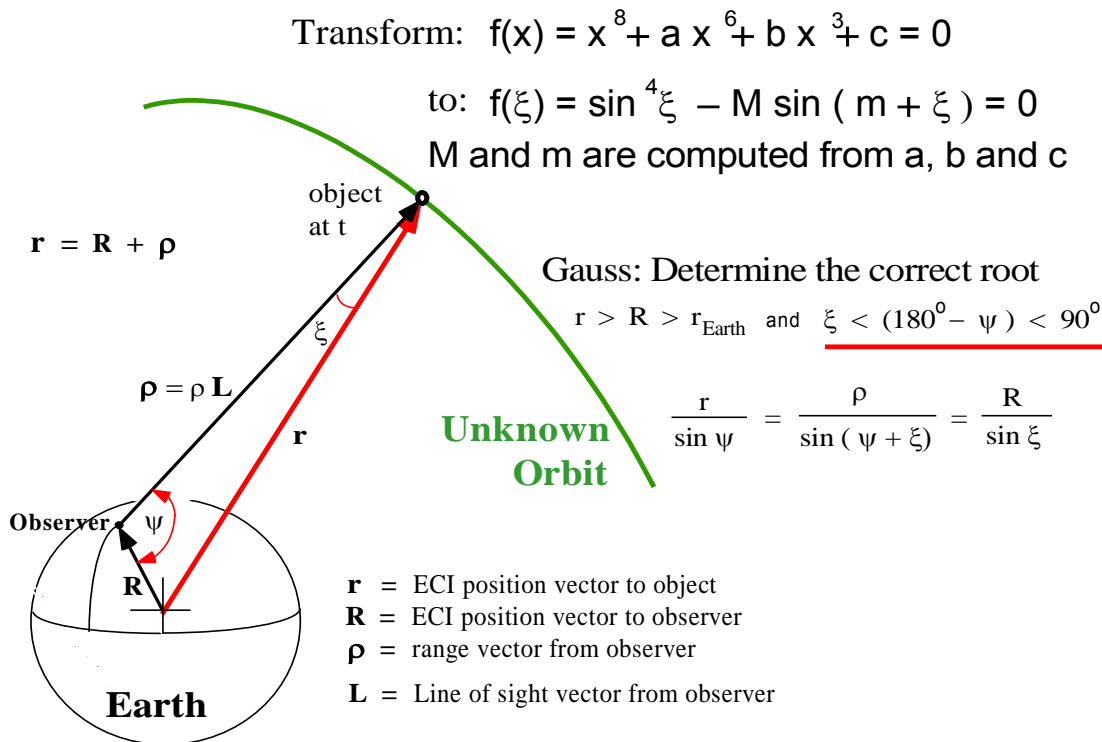


Figure 2. Gauss geometric method

2.2 Gauss Geometric Method

As described in [21], Gauss transformed Equation (1) to:

$$f(\xi) = \sin^4 \xi - M \sin(m + \xi) = 0 \quad (2)$$

where M and m are constants computed from the angles-only inputs, and the unknown ξ is the angle between the position vectors $\boldsymbol{\rho}$ and \mathbf{r} as shown in Figure 2. Theoretically, any visible object must lie above the ground observer's horizon, implying that $90^\circ < \psi < 180^\circ$ and $0 \leq \xi < 90^\circ$. The Gauss geometric method also uses the Law of Sines as:

$$\frac{r}{\sin \psi} = \frac{\rho}{\sin(\psi + \xi)} = \frac{R}{\sin \xi} \quad (3)$$

to relate the magnitudes of the three position vectors, \mathbf{r} , $\boldsymbol{\rho}$, and \mathbf{R} , after ξ is found. The correct root that corresponds to the real unknown orbit must satisfy:

$$\left. \begin{array}{l} r_{\text{Earth}} < R < r \\ 0 < \xi < (180^\circ - \psi) < 90^\circ \end{array} \right\} \quad (4)$$

For an orbiting space sensor of Geocentric IOD (and Heliocentric IOD in Celestial Mechanics), at most two other roots may exist, but they are associated with $\xi \geq 90^\circ$. By not allowing the line of sight to see through the Earth, one of the two possible roots can often be eliminated. Other intuitive relations may be needed.

2.3 A Simple Iterative Method for Equations (1) and (2)

Supposing the search is for an Earth satellite or an orbital debris object by a ground sensor, the starting magnitude of the Cartesian or Earth Centered Inertial (ECI) position vector is $x_1 = |\mathbf{r}(t_2)| = r_{\text{Earth}}$ for Equation (1). The iterative method, which assume no a priori knowledge, may end at any desired range limit, say 100,000 km for Geocentric IOD with a step of 500 km. Since the altitude of 90% of the Space objects around the Earth are about 2,000 km or less, the solution of a Near Earth object can be found in a few steps. If there are three positive real roots, Gauss geometric method is required. The starting value of ξ is zero for Equation (2), and the maximum value is 90° for ground sensors. The confusion of multiple roots begins with $0 \leq \xi \leq 180^\circ$, and only applies to orbiting space sensors and Heliocentric IOD. If the evaluation of ξ is separated between $0 \leq \xi \leq 90^\circ$ and $90^\circ < \xi \leq 180^\circ$, finding the correct ξ and then x of Equation (1) is intuitive.

3. A New Double-r Algorithm

Two arbitrary starting values and a non-robust iterative method (Newton-Raphson) are problematic for the traditional Double-r algorithms. Even though range guessing is replaced by range solving, forcing their target functions to convergence is tricky when high-order partial derivatives, multi-dimensional matrix inversions and sensitive iterative methods are involved.

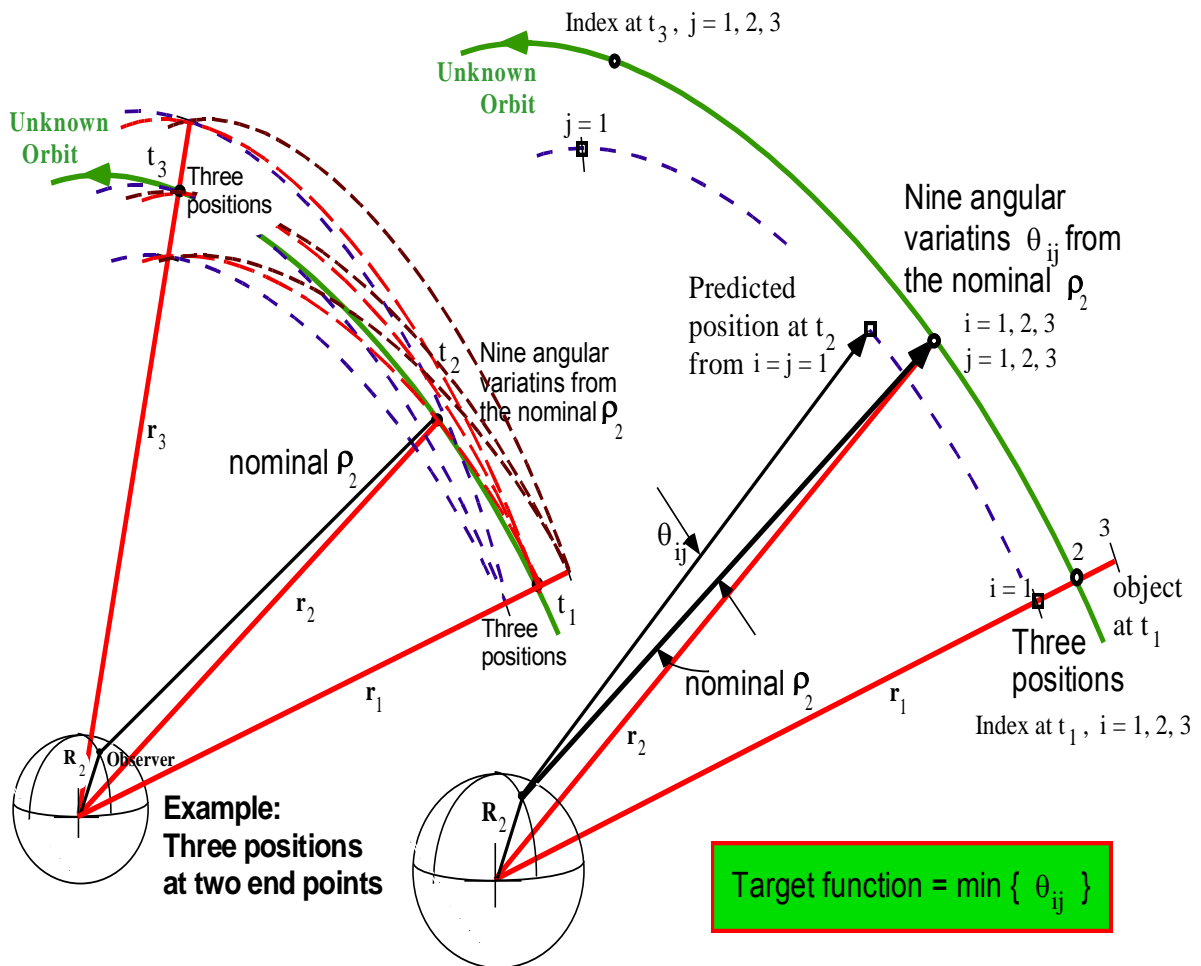


Figure 3. Range solving and Lambert targeting of the new Double-r algorithm

With the two reasonably accurate initial range estimates at points 1 and 3 provided by range solving, Lambert targeting with analytic perturbed trajectories [27] and [28], becomes possible. As shown in the left of Figure 3, the two initial range estimates of Gauss or Laplace at points 1 and 3 can be varied, and multiple Lambert solutions between the end points 1 and 3 can be easily computed. In the right of Figure 3, the simple target function is θ_{ij} , the angle between the given nominal line-of-sight vector ρ_2 and the ECI position vector computed by Lambert targeting at point 2. The optimum ranges, r_i and r_j , at respectively points 1 and 3 are those associated with the 2-dimensional minimum θ_{ij} . If ρ_2 is allowed to vary, a 3-dimensional minimum θ_{ij} can often be found to be smaller than the 2-dimensional one. The analytic perturbed or post-Keplerian trajectories with $(J_2, J_3, J_4, \text{Sun, Moon, } \dots)$ can be replaced by those from numerical integration, if higher accuracy instead of speed is desired. The variations of θ_{ij} provide a view of the optimum solution. The comparison of the Double-r algorithms of the author and a version of Gooding [18] is illustrated in Figure 4.

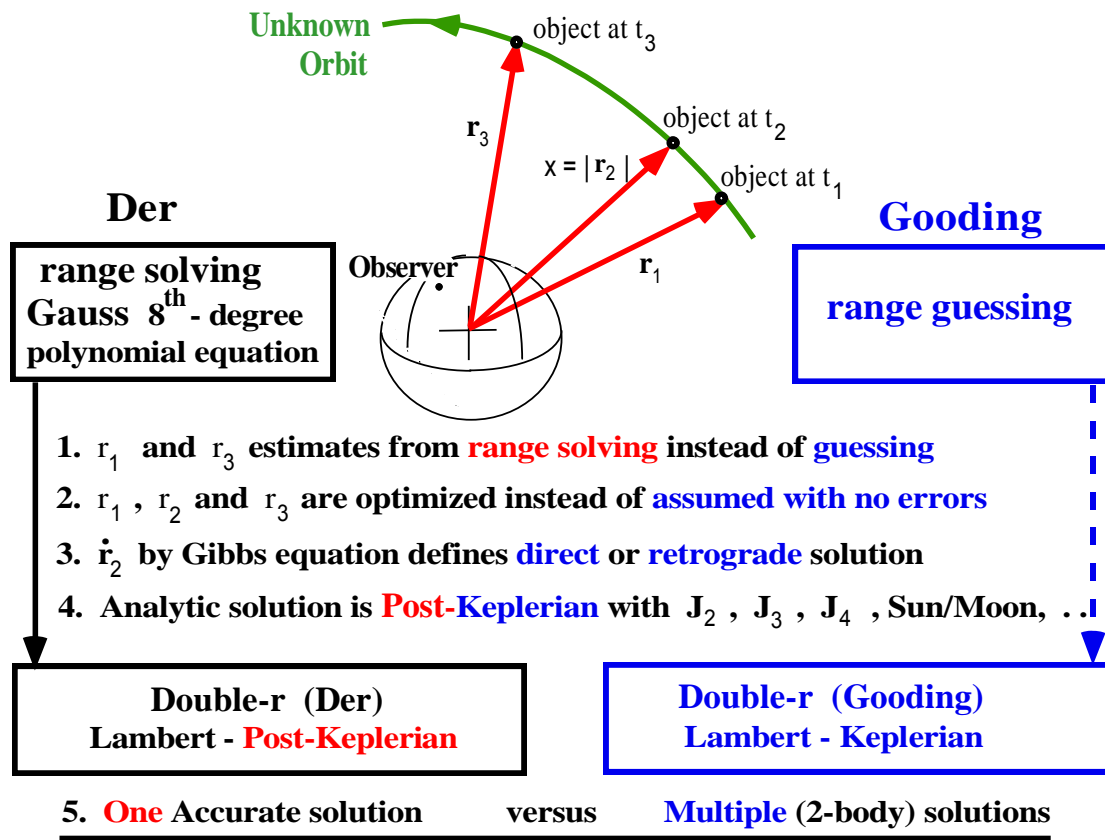


Figure 4. Double-r algorithms comparison

4. Numerical Examples

For Geocentric orbits, the Space Catalog provides initial state vectors for objects at different orbit regimes. For Heliocentric orbits, the state vectors of most planetary objects can be extracted from the JPL DE405 ephemeris file and the Minor Planet file of International Astronomical Union (IAU) for almost any date. These accurate Geocentric and Heliocentric state vectors form the “error-free” reference IOD solutions for all practical purposes.

How accurate does the angles data have to be? In the following ten examples, the estimated ranges x 's and coefficients a , b , and c of Equation (1) from both the Gauss and Laplace algorithms are given for objects at different orbit regimes as well as various eccentricities, inclinations and locations on the orbits. The reader can verify that Equation (1), $f(x) = x^8 + a x^6 + b x^3 + c = 0$, is indeed satisfied with the set, (x, a, b, c) , of each example. Accurate input angles give accurate coefficients, which in turn produce reasonable range estimates. Reasonable means that the estimated range is within five percent of the desired range at t_2 . Note that, x is normalized with the Earth radius of 6378.137 km or AU of 149597870.691 km.

In practice, the most likely source of errors of optical sensors and optical telescopes is usually the angles observation data. Time error is insignificant due to the use of atomic clocks in operational sensors. If real observation data is not available, then other means of injecting errors are needed for robustness evaluations of the algorithms. Since error-free angles data can be computed with the use of the Space Catalog and the JPL DE405 ephemeris file, “angular measurement errors” can be introduced systematically. On the other hand, inaccurate angles data of asteroids and comets from most Astronomy magazines are unable to produce accurate coefficients of Equation (1), and the resulting estimated ranges do not match even within 90% percent of those known reference solutions. The characteristics of angular errors and estimated ranges of Equation (1) are illustrated as follows:

Input angles data	Number of accurate significant digits in the angles data	Example: Right ascension or Declination (degrees)	Expected % of errors	Estimated range
Error-free	5 or more	12.345 or more	1 or less	excellent
Marginal	3 or 4	12.3 or 12.34	2 to 5	good to poor
Inaccurate	2 or less	12. or less	>> 5	unacceptable

More than a hundred objects and six hundred test cases were analyzed with and without measurement errors. The position and velocity vectors computed by the new Gauss, Laplace and Double-r angles-only algorithms are compared with the answers. Ten sample examples for Geocentric and Heliocentric IOD were chosen and the estimated Gauss / Laplace parameters: x, eccentricity and inclination are summarized as follows:

Example	Input errors (%)	Estimated Gauss / Laplace Parameters		
		x= ECI - SCI range (km)	Eccentricity	Inclination (deg)
1. Geocentric, MEO	0	9037 / 9503	0.08 / 0.15	32.4 / 32.1
2. Geocentric, Molniya	0	41200 / 41201	0.75 / 0.75	26.5 / 26.5
3. Geocentric, GEO	0	41856 / 41892	0.02 / 0.02	0.32 / 0.32
4. Geocentric, LEO	0.1	7367 / 7496	0.05 / 0.03	82.8 / 82.5
5. Geocentric, HEO	0.1	20558 / 20575	0.096 / 0.095	125. / 125.
6. Geocentric, MEO	0.1	8757 / 8954	0.24 / 0.19	105. / 105.
7. Geocentric, MEO	Text-Book	10480 / 12769	0.16 / 1.47	40. / 39.
8. Heliocentric, Saturn	0	1450559175 / 1450394230	0.055 / 0.059	22.5 / 22.5
9. Heliocentric, Jupiter	0.1	782628237 / 236738371	0.042 / 0.904	23.2 / 23.0
10. Heliocentric, Ceres	0.1	422629637 / 471776591	0.102 / 0.318	27.2 / 28.0

In general, the solutions of Laplace in Examples 1 to 10 are not as accurate as those of Gauss. As indicated in [16], the Laplace algorithm requires topocentric correction, while the Gauss algorithm handles topocentric observation data naturally. Since the new algorithms are range independent, solutions are not affected by input data from multiple sensors or observers. In the following examples, only one observer is used. The results of the new algorithms are colored in red, and the desired answer in green in the Tables.

Example 1. MEO, error-free

Descartes' Rule of Signs indicates one positive real root for both Gauss and Laplace, and can be found as shown in Section 2. The converged ECI position and velocity vectors of the new Double-r (Lambert targeting) algorithm are much closer to those of the unknown orbit than both the Gauss and Laplace algorithms as shown in Table 1.

Given:

Ground Sensors	Latitude (deg)	Longitude (deg)	Altitude (km)
Sites 1, 2, 3	39.13607	-121.35072	0.09981638

Date (yr/mo/dd/hr/min/sec)	Right ascension (deg)	Declination (deg)
2009/ 5/ 26/ 16/ 0/ 20.475	309.340542	0.660969
2009/ 5/ 26/ 16/ 10/ 20.475	358.990622	-20.660902
2009/ 5/ 26/ 16/ 20/ 20.475	41.951457	-36.687800

Output comparison of the three new algorithms

estimated Gauss coefficients (a = -0.9947, b = -1.7702, c = -3.1618)

estimated Laplace coefficients (a = -0.9917, b = -4.7278, c = -5.6107)

$t_2 = t_1 + 600$ seconds	ECI position vector (km)			ECI velocity vector (km/s)		
Gauss	8644.17	417.46	2603.42	0.5702	5.6572	-2.8880
Laplace	9186.35	407.90	2398.94	0.8789	5.3049	-2.7071
Double-r (targeting)	8796.02	446.97	2530.72	0.6336	5.8421	-3.0196
Answer	8794.68	414.81	2546.67	0.5903	5.8483	-2.9933

Table 1. Comparison of solutions of the new algorithms for MEO at t_2

Example 2. Molniya, error-free

Descartes' Rule of Signs indicates one positive real root for both Gauss and Laplace. All the solutions from the Gauss, Laplace and Double-r (targeting) algorithms are close to the unknown Molniya orbit as shown in Table 2.

Given:

Ground Sensors	Latitude (deg)	Longitude (deg)	Altitude (km)
Sites 1, 2, 3	30.5724	-86.2143	0.0

Date (yr/mo/dd/hr/min/sec)	Right ascension (deg)	Declination (deg)
2011/ 1/ 4/ 13/ 0/ 46.5	280.040780	-31.377194
2011/ 1/ 4/ 13/ 5/ 46.5	280.896316	-31.544420
2011/ 1/ 4/ 13/ 10/ 46.5	281.776909	-31.712006

Output comparison of the three new algorithms

estimated Gauss coefficients (a = -1.0009, b = -191.958, c = -2907201.2)

estimated Laplace coefficients (a = -1.0024, b = -273.755, c = -2907697.5)

$t_2 = t_1 + 300$ seconds	ECI position vector (km)			ECI velocity vector (km/s)		
Gauss	1977.66	-37012.56	-17990.31	1.6270	1.6112	0.5453
Laplace	1977.82	-37013.40	-17990.84	1.6273	1.6120	0.5455
Double-r (targeting)	1977.66	-37012.56	-17990.31	1.6270	1.6112	0.5453
Answer	1977.27	-37010.52	-17989.04	1.6269	1.6111	0.5452

Table 2. Comparison of solutions of the new algorithms for Molniya at t_2

Example 3. GEO, error-free

Descartes' Rule of Signs indicates three positive real roots for Gauss; two with the LEO ranges and one GEO range. However, The Gauss geometric method deduced a range near GEO, and therefore the correct range is that of the GEO.

Given:

Ground Sensors	Latitude (deg)	Longitude (deg)	Altitude (km)
Sites 1, 2, 3	30.5724	-86.2143	0.0

Date (yr/mo/dd/hr/min/sec)	Right ascension (deg)	Declination (deg)
2006/ 9/ 11/ 4/ 45/ 44.073	17.473272	-5.246774
2006/ 9/ 11/ 4/ 50/ 44.073	18.725895	-5.245155
2006/ 9/ 11/ 4/ 55/ 44.073	19.978504	-5.243423

Output comparison of the three new algorithms

estimated Gauss coefficients ($a = -0.6590$, $b = 343.975$, $c = -3506478.8$)

estimated Laplace coefficients ($a = 0.1447$, $b = -1864.78$, $c = -3508165.1$)

$t_2 = t_1 + 300$ seconds	ECI position vector (km)			ECI velocity vector (km/s)		
Gauss	40702.37	9900.55	-231.49	-0.7182	2.9675	0.0034
Laplace	40704.75	9901.36	-231.72	-0.7182	2.9674	0.0034
Double-r (targeting)	40704.75	9901.36	-231.72	-0.7183	2.9676	0.0034
Answer	40325.23	12355.73	-153.49	-0.8999	2.9391	0.0036

Table 3. Comparison of solutions of the new algorithms for GEO at t_2

Example 4. LEO, with 0.1% angular errors

A piece of rocket body in LEO at a very high inclination and the addition of 0.1% angular measurement errors did not cause any problem for range solving. Laplace solution is sensitive to angular errors.

Given:

Ground Sensors	Latitude (deg)	Longitude (deg)	Altitude (km)
Sites 1, 2, 3	39.0072	-104.8810	0.0

Date (yr/mo/dd/hr/min/sec)	Right ascension (deg)	Declination (deg)
2011/ 1/ 18/ 10/ 9/ 54.0	224.8542	-0.5230
2011/ 1/ 18/ 10/ 12/ 28.0	209.4250	32.3940
2011/ 1/ 18/ 10/ 14/ 44.0	179.6625	55.5490

Output comparison of the three new algorithms:

estimated Gauss coefficients (a = -0.9964, b = -0.4134, c = -0.1647)

estimated Laplace coefficients (a = -0.9950, b = -0.9716, c = -0.2271)

$t_2 = t_1 + 154$ seconds	ECI position vector (km)			ECI velocity vector (km/s)		
Gauss	-31.5	-5510.0	4889.7	1.2842	4.8883	5.5881
Laplace	-172.1	-5589.3	4992.1	1.4051	4.7646	5.2211
Double-r (targeting)	-30.9	-5510.5	4889.3	1.2881	4.8888	5.5822
Answer	-14.5	-5504.8	4880.2	1.2167	4.8075	5.4409

Table 4. Comparison of solutions of the new algorithms for LEO at t_2

Example 5. HEO, with 0.1% angular errors

An object in HEO in a retrograde orbit of inclination 125 degrees and the addition of 0.1% angular measurement errors also did not cause any problem for range solving.

Given:

Ground Sensors	Latitude (deg)	Longitude (deg)	Altitude (km)
Sites 1, 2, 3	30.5724	-86.2143	0.0

Date (yr/mo/dd/hr/min/sec)	Right ascension (deg)	Declination (deg)
2011/ 1/ 4/ 21/ 42/ 20.796	12.8101	-12.1200
2011/ 1/ 4/ 21/ 47/ 20.796	9.4820	-8.1840
2011/ 1/ 4/ 21/ 52/ 20.796	6.1085	-4.1066

Output comparison of the three new algorithms:

estimated Gauss coefficients (a = -1.7861, b = -152.5439, c = -4538.25)

estimated Laplace coefficients (a = -2.3968, b = -248.2428, c = -4565.19)

$t_2 = t_1 + 300$ seconds	ECI position vector (km)			ECI velocity vector (km/s)		
Gauss	20503.9	1095.3	1008.8	0.0206	-2.6703	3.7548
Laplace	20521.4	1098.2	1006.2	0.0166	-2.6691	3.7525
Double-r (targeting)	20155.4	1036.4	1060.6	0.0395	-2.5970	3.6657
Answer	19966.4	1005.7	1086.9	0.1035	-2.5788	3.6356

Table 5. Comparison of solutions of the new algorithms for HEO at t_2

Example 6. MEO, with 0.1% angular errors

An MEO object in a retrograde orbit of inclination 105 degrees and the addition of 0.1% angular measurement errors also did not cause any problem for range solving.

Given:

Ground Sensors	Latitude (deg)	Longitude (deg)	Altitude (km)
Sites 1, 2, 3	30.5724	-86.2143	0.0

Date (yr/mo/dd/hr/min/sec)	Right ascension (deg)	Declination (deg)
2011/ 1/ 5/ 0/ 3/ 37.058	19.6005	-49.2810
2011/ 1/ 5/ 0/ 8/ 37.058	6.8133	-21.8569
2011/ 1/ 5/ 0/ 13/ 37.058	354.1102	11.9095

Output comparison of the three new algorithms:

estimated Gauss coefficients (a = -0.9946, b = -1.5932, c = -1.8436)

estimated Laplace coefficients (a = -0.9900, b = -3.6647, c = -2.4270)

$t_2 = t_1 + 300$ seconds	ECI position vector (km)			ECI velocity vector (km/s)		
Gauss	8223.3	2262.9	1987.1	0.5968	-1.7360	6.5272
Laplace	8446.8	2289.6	1896.8	0.3750	-1.7159	6.3889
Double-r (targeting)	8256.9	2267.6	1972.7	0.6033	-1.7577	6.5941
Answer	8209.2	2261.3	1993.4	0.5708	-1.7319	6.4897

Table 6. Comparison of solutions of the new algorithms for LEO at t_2

Example 7 MEO, with angular errors

Example 7 compares the traditional and new Gauss, Laplace and Double-r angles-only algorithms for a MEO object. The traditional algorithms produce Keplerian solutions and those of the new algorithms include J_2 , J_3 , J_4 , Sun, Moon, and other perturbations when applicable. As expected, the post-Keplerian initial orbits of the new algorithms are more accurate for the unknown MEO object. The Laplace solutions are problematic due to the inaccurate derivatives of the line-of-sight vectors and the lack of topocentric correction.

Given:

Ground Sensors	Latitude (deg)	Longitude (deg)	Altitude (km)
Sites 1, 2, 3	40.00	-110.00	2.0

Date (yr/mo/dd/hr/min/sec)	Right ascension (deg)	Declination (deg)
2007/ 8/ 20/ 11/ 40/ 0.	-0.4173	17.4627
2007/ 8/ 20/ 11/ 50/ 0.	55.0932	36.5732
2007/ 8/ 20/ 12/ 20/ 0.	134.2827	12.0351

Output comparison of the traditional Gauss and the new Gauss algorithms:

estimated Gauss coefficients (a = -1.0536, b = -5.5411, c = -7.8042)

$t_2 = t_1 + 600$ seconds	ECI position vector (km)			ECI velocity vector (km/s)		
Gauss (traditional, knew answer)	6195.2	6054.0	6960.4	-4.3983	4.5907	1.4902
Gauss (traditional, range guessing)	5258.1	5219.5	5968.2	-3.8035	4.9485	1.9484
Gauss (range solving)	5892.3	5638.1	6581.2	-4.2548	4.4931	1.4804
Answer	5963.6	5722.1	6660.2	-4.3643	4.6055	1.5157

Table 7a. Comparison of the traditional and new Gauss algorithms at t_2

Output comparison of the traditional Laplace and the new Laplace algorithms:

estimated Laplace coefficients (a = -1.3911, b = -29.9691, c = -54.7061)

$t_2 = t_1 + 600$ seconds	ECI position vector (km)			ECI velocity vector (km/s)		
Laplace (traditional, knew answer)	3974.9	2872.1	4081.8	-54.186	76.955	4.2796
Laplace (traditional, range guessin)	3973.5	2871.2	4080.4	-52.368	75.748	4.0635
Laplace (new range solving)	6956.0	7162.3	7960.3	-4.3379	7.0773	3.2628
Answer	5963.6	5722.1	6660.2	-4.3643	4.6055	1.5157

Table 7b. Comparison of the traditional and new Laplace algorithms at t_2

Output comparison of the traditional Double-r and the new Double-r algorithms:

$t_2 = t_1 + 600$ seconds	ECI position vector (km)			ECI velocity vector (km/s)		
Double-r (traditional, knew answer)	5963.6	5722.1	6660.2	-4.3643	4.6055	1.5157
Double-r (traditional, range guess)	5465.5	5598.6	6273.0	3.3737	-3.2997	-0.7452
Double-r (new Lambert-targeting)	5986.8	5731.9	6675.1	-4.4079	4.6154	1.5083
Answer	5963.6	5722.1	6660.2	-4.3643	4.6055	1.5157

Table 7c. Comparison of the traditional and new Double-r algorithms at t_2

Example 8. Saturn, error-free

The state vectors of the Earth (observer) and Saturn (unknown object) were obtained from the DE405 ephemeris file. Since DE405 data is sufficiently accurate, the coefficients of the *Equations* are computed accurately and the resulting range estimates show less than 0.01 percent of error. Numerous test cases similar to this show that the angles data generated from state vectors of DE405 can be considered error-free for Heliocentric IOD.

Given:

Date (yr/mo/dd/hr/min/sec)	Sun Centered Inertial (SCI) position vector of Earth (km)		
2012/ 1/ 5/ 0/ 0/ 0	-35255503.218	131027107.594	56802595.735
2012/ 1/ 15/ 0/ 0/ 0	-59975833.469	123279624.956	53444542.024
2012/ 1/ 25/ 0/ 0/ 0	-82851903.993	111707451.012	48426993.723

Date (yr/mo/dd/hr/min/sec)	Right ascension (deg)	Declination (deg)
2012/ 1/ 5/ 0/ 0/ 0	207.225236	-8.612771
2012/ 1/ 15/ 0/ 0/ 0	207.702672	-8.746206
2012/ 1/ 25/ 0/ 0/ 0	208.025024	-8.819056

Output comparison of the three new algorithms:

estimated Gauss coefficients (a = -94.2131, b = 176.2090, c = -83.2408)

estimated Laplace coefficients (a = -92.5929, b = 177.4249, c = -85.8668)

$t_2 = 2012/ 1/ 5/ 0/ 0/ 0$	SCI position vector (km)			SCI velocity vector (km/s)		
Gauss	-1333576603.	-545451505.	-167863101.	3.25018	-8.17905	-3.51824
Laplace	-1333432206.	-545373845.	-167837250.	3.23104	-8.14597	-3.50334
Double-r (targeting)	-1333587737.	-545455511.	-167864277.	3.25122	-8.17857	-3.51809
Answer	-1333553680.	-545439469.	-167859117.	3.25175	-8.17798	-3.51788

Table 8. Comparison of solutions of the new algorithms for Saturn at t_2

Example 9. Jupiter, errors in both Earth position and measurement angles

The state vectors of the Earth (observer) and Jupiter (unknown object) were obtained from the DE405 ephemeris file. Only the first four digits of each component of the Earth position vector were kept, and about 0.1% angular measurement errors were added to the

given angles. Even though the injected errors produced substantial differences in the coefficients of *the Equations* with respect to the error-free set, the resulting solutions of Gauss and Double-r are still reasonable. The Laplace solution is poor due more to inaccurate angles data than the lack of topocentric correction.

Given:

Date (yr/mo/dd/hr/min/sec)	Sun Centered Inertial (SCI) position vector of Earth (km)		
1990/ 1/ 13/ 0/ 0/ 0	-21506189.890	133516099.591	57889888.021
1990/ 6/ 22/ 0/ 0/ 0	-33904861.413	-135786995.268	-58874242.010
1991/ 1/ 8/ 0/ 0/ 0	-7825464.615	134802641.279	58447888.078

Date (yr/mo/dd/hr/min/sec)	Right ascension (deg)	Declination (deg)
1990/ 1/ 13/ 0/ 0/ 0	96.1155	23.1980
1990/ 6/ 22/ 0/ 0/ 0	105.6750	22.8340
1991/ 1/ 8/ 0/ 0/ 0	135.3780	17.6250

Output comparison of the three new algorithms:

estimated Gauss coefficients (a = -26.9859, b = -54.6752, c = -27.9185)

estimated Laplace coefficients (a = -5.1060, b = 109.8792, c = -411.8757)

desired DE405 coefficients (a = -22.2869, b = -640.2321, c = -4616.1931)

t ₂ =1990/ 6/ 22/ 0/ 0/ 0	SCI position vector (km)			SCI velocity vector (km/s)		
Gauss	-261600740.	675625800.	295975993.	-12.52795	-3.70017	-1.28055
Laplace	-123833006.	184676217.	81271996.	-7.10912	-2.34991	-0.83643
Double-r (targeting)	-260704051.	672287708.	294525001.	-12.49367	-3.56258	-1.22239
Answer	-275779769.	668036623.	293070634.	-12.40066	-3.80315	-1.32804

Table 9. Comparison of solutions of the new algorithms for Jupiter at t₂

Example 10. Ceres, no error in Earth position (DE405) and 0.1% errors in angles

The state vectors of the Earth (observer) were obtained from the DE405 ephemeris file. The angles data of the Asteroid, Ceres, (unknown object) were obtained from the IAU Minor Planet file, and then about 0.1% of the angles values were injected. Again, the resulting solutions of Gauss and Double-r are reasonable, and that of Laplace is slightly worse (no topocentric correction) as compared to the reference or error-free solution.

Given:

Date (yr/mo/dd/hr/min/sec)	Sun Centered Inertial (SCI) position vector of Earth (km)		
2007/ 9/ 21/ 11/ 0/ 0	150086429.982	-5920069.652	-2566523.573
2007/ 11/ 16/ 8/ 21/ 0	88770118.835	108605877.253	47084078.714
2007/ 12/ 27/ 20/ 28/ 0	-12113351.966	134518218.510	58317762.754

Date (yr/mo/dd/hr/min/sec)	Right ascension (deg)	Declination (deg)
2007/ 9/ 21/ 11/ 0/ 0	53.8530	9.3300
2007/ 11/ 16/ 8/ 21/ 0	45.2650	7.9900
2007/ 12/ 27/ 20/ 28/ 0	38.9830	9.2900

Output comparison of the three new algorithms:

estimated Gauss coefficients ($a = -8.3070$, $b = 7.4193$, $c = -1.6649$)

estimated Laplace coefficients ($a = -14.8667$, $b = 22.2634$, $c = -7.0259$)

estimated reference coefficients ($a = -8.2687$, $b = 7.3762$, $c = -1.6532$)

$t_2 = 2007/11/16/8/21/0$	SCI position vector (km)			SCI velocity vector (km/s)		
Gauss	281643924.	303272115.	85548432.	-13.77172	8.40280	6.86640
Laplace	315978300.	337925797.	92396002.	-15.79460	6.04161	6.44416
Double-r (targeting)	281639476.	303278630.	85554626.	-13.77296	8.40357	6.86610
Answer	280939236.	302533514.	85416262.	-13.74141	8.48263	6.87925

Table 10. Comparison of solutions of the new algorithms for Ceres at t_2

Conclusions

This paper presents three new angles-only IOD algorithms that can consistently deduce the correct range or root of the Gauss or Laplace eighth-degree polynomial equations without guesswork for any unknown object in any orbit regime, and therefore the 200-year angles-only problem is solved. The Keplerian (2-body) solution is then analytically extended to include perturbations for speed and accuracy.

These new angles-only algorithms have been further improved to meet more accurate cataloging and correlation requirements of the Space Based Space Surveillance and the Space Fence systems, while also provide the needed algorithms for all manner of Real-Time Space Situational Awareness.

References

1. Gauss, C.F. "Theory of Motion of the Heavenly Bodies Moving About the Sun in Conic Sections", 1809, (English translation, Dover Phoenix Editions).
2. F.R. Moulton, "An Introduction to Celestial Mechanics", The Macmillan Company, New York, 1914
3. Escobal, P.R., "Methods of Orbit Determination", Robert E. Krieger Publishing Company, Malabar, Florida, USA, 1965.
4. Herrick, S., "Astrodynamics", Vol 1, Van Nostrand Reinhold, London, 1971.
5. Bate, R., and Mueller, D., and White, W., "Fundamentals of Astrodynamics", Dover Publications, Inc., Toronto, Canada, 1971.
6. Battin, R.H. "An Introduction to The Mathematics and Methods of Astrodynamics", American Institute of Aeronautics and Astronautics, Education Series, 1987
7. D. Vallado, D. and McClain, W.D., "Fundamentals of Astrodynamics and Applications", (1st, 2nd, 3rd Editions), 1997, 2001
8. Montenbruck, O. and Gill, O., "Satellite Orbits", Springer Verlag, 2000.
9. Prussing, J.E., Conway, B.A., "Orbital Mechanics", Oxford University, 1993.

10. Briggs, R.E., Slowey, J.W., "An Iterative Method of Orbit Determination from Three Observations of a Nearby Satellite", Astrophysical Observatory, Smithsonian Institution, 1959.
11. Taff, L.G., et al, "Angles-only, Ground-Based, Initial Orbit Determination", Lincoln Laboratory, MIT, 1984.
12. Marsden, B.G., "Initial Orbit Determination: The Pragmatists Point of View", *Astronomical Journal*, 1985
13. Long, Anne C. et al., "Goddard Trajectory Determination System (GTDS) Mathematical Theory (Revision 1)". FDD/552-89/001 and CSC/TR-89/6001, Goddard Space Flight Center: National Aeronautics and Space Administration, 1989.
14. Kaya, D.A. and Snow, D.E., "Short Arc Initial Orbit Determination using Angles-only Space Based Observations", AIAA, AAS 91-358, 1991.
15. Gooding, R.H. "A New Procedure for Orbit Determination based on three Lines of Sight (Angles only)", Defence Research Agency, TR93004, 1993.
16. Milani, A. et al, "Topocentric Orbit Determination: Algorithms for the Next Generation Surveys", *Icarus* 195, 1, 2008.
17. Vallado, D.A., "Evaluating Gooding Angles-only Orbit Determination of Space Based Space Surveillance Measurements", AAS 10-xxx, Born, 2010.
18. SchaeperKoetter, A.V., "A Comprehensive Comparison Between Angles-only Initial Orbit Determination Techniques", MS Thesis, Texas A&M U, December 2011.
19. Fadrique, F.M. et al, "Comparison of Angles only Orbit Determination Algorithms for Space Debris Cataloguing", <http://www.gmv.com/export/.../2011...pdf>
20. Charlier, C.V. L., "On Multiple Solutions in the Determination of Orbits from Three Observations", *MNRAS* 71, 120-124, 1910; *MNRAS* 71,454-459, 1911.
21. Plummer, H.C., "An Introductory Treatise on Dynamical Astronomy", Cambridge University Press, 1918.
22. Demars, K.J., Jah, M.K., Schumacher, P.W. Jr., "The Use of Short-Arc Angle and Angle Rate Data for Deep-Space Initial Orbit Determination and Track Association", 2011.
23. Kelecy, T., Jah, M.K., DeMars, K.J., "Application of Multiple Hypothesis Filter to Near GEO High Area-to-Mass Ratio Space Objects State Estimation", 62 International Astronautical Congress, Cape Town, SA, 2011.
24. Horwood, J., Poore, A.B., Alfriend, K.T., "Orbit Determination and Data Fusion in GEO", AMOS, Maui, Hawaii, 2011.
25. Faccenda, W.J. et al, "Deep Stare Technical Advancements and Status", MITRE Report, 2003.
26. Levin, S.A., "Descartes' Rule of Signs – How hard can it be?", sepwww.stanford.edu/oldsep/stew/descartes.pdf, 2002.
27. Der, G.J., "The Superior Lambert Algorithm", AMOS, Maui, Hawaii, 2011.
28. Vinti, J.P., "Orbital and Celestial Mechanics", AIAA, Volume 177, 1998